Neurourology and Urodynamics 15:235–248 (1996)

Morphometric Data of Canine Sacral Nerve Roots With Reference to Electrical Sacral Root Stimulation

Nico J.M. Rijkhoff, Evert L. Koldewijn, Wendy d'Hollosy, Frans M.J. Debruyne, and Hessel Wijkstra

Department of Urology, University Hospital Nijmegen, The Netherlands

Experiments to investigate restoration of lower urinary tract control by electrical stimulation of the sacral nerve roots are mostly performed on dogs, yet little morphometric data (such as canine root and fiber diameter distributions) are available. The aim of this study was to acquire morphometric data of the intradural canine sacral dorsal and ventral roots (S1-S3). Cross-sections of sacral roots of two beagle dogs were analyzed using a light microscope and image processing software. The cross-sectional area of each root was measured. The diameters of the fibers and the axons in the cross-sections of the S2 and S3 roots were measured and used to construct nerve fiber diameter frequency distribution histograms. The results show a unimodal diameter distribution for the dorsal roots and a bimodal distribution for the ventral roots. In addition the average ratio g of the axon diameter to fiber diameter was calculated for each root. © 1996 Wiley-Liss, Inc.

Key words: dog, sacral nerve root, electrical stimulation, fiber diameter distribution

INTRODUCTION

Patients with neuropathic voiding disorders are at risk for urinary tract infections and kidney damage. To restore bladder control, an increasing number of patients are treated with electrical stimulation of the sacral nerve roots using implanted electrodes. Two different patient groups can be distinguished. The first group consists of patients with idiopathic voiding disorders who do not successfully respond to conventional treatments. Spinal cord injury patients form the second group. For patients with idiopathic disorder, a quadripolar wire electrode is implanted in one of the sacral foramina close to a sacral root and connected to a

Received for publication May 31, 1995; accepted December 6, 1995.

Address reprint requests to Dr. Nico J.M. Rijkhoff, Department of Urology, University Hospital Nijmegen, P.O. Box 9101, 6500 HB Nijmegen, The Netherlands.

subcutaneous stimulator [Schmidt, 1988; Siegel, 1992]. The stimulator is always on, except at the time of micturition. Stimulation of the roots is regarded in this group as a long-term therapeutic treatment. The success rate of the therapy is rather low and reasons for this low success rate are unknown since it is still unclear how stimulation of the nerve roots can improve voiding disorders [Koldewijn et al., 1994].

Spinal cord patients have lost their volitional bladder control and suffer from detrusor hyperreflexia and detrusor-sphincter dyssynergia. One of the current approaches is twofold: deafferentation by dorsal sacral rhizotomies eliminates the reflex detrusor contractions while voiding is induced by stimulation of the ventral sacral nerve roots to activate the detrusor [Brindley et al., 1986; van Kerrebroeck et al., 1991]. However, the selectivity of this stimulation technique is insufficient. Both the urethral sphincter and the detrusor are simultaneously activated, resulting in little or no voiding. In clinical practice this problem is overcome by interrupting the stimulus pulse train. As the striated muscle of the urethral sphincter relaxes faster after a stimulus burst than the smooth detrusor muscle, bladder emptying is achieved between the pulse trains due to the sustained high intravesical pressure. However, in this artificial micturition pattern voiding occurs in spurts with possible supranormal intravesical pressures. The latter could be harmful to the kidneys.

To increase the success rate of the stimulator implants and to improve the stimulation techniques, research is carried out at various levels. Traditionally, improvements in stimulation strategy and electrode configurations rely mainly on animal experiments (dogs) [Schmidt et al., 1979; Thüroff et al., 1982; Sweeney et al., 1990; Li et al., 1992; Hohenfellner et al., 1992; Ishigooka et al., 1994; Rijkhoff et al., 1994b] and clinical testing. However, to obtain insight into the effects of electrical stimulation and to optimize stimulation patterns, computer models have also become available [Hosein and Griffiths, 1990; Rijkhoff et al., 1994a].

For several reasons, data of the nerve roots are needed when developing stimulation strategies. To obtain realistic simulation results with the computer model developed by Rijkhoff et al. [1994a], the electrical properties and the dimensions of nerve roots must be incorporated. In addition, the properties of the myelinated nerve fiber determining its electrical behavior (e.g., fiber diameter) must be known. To quantitatively compare experimental data with theoretical simulation results, anatomical sacral root data are also needed. Moreover, to transfer an application successfully from animal experiments to patients, differences between animal and human sacral roots must be known. Anatomical sacral root data would also be valuable for researchers working on nerve anastomosis as another method to restore bladder function in paraplegia [Carlsson and Sundin, 1980; Schalow, 1992a].

Human sacral root data have been published by Schalow [1985, 1989, 1992a], and although the dog is the most used animal in sacral root stimulation research, little data of the canine sacral nerve roots have been published [Schalow and Barth, 1992]. To acquire data of canine sacral nerve roots, we removed the intradural sacral roots of two dogs and analyzed cross-sections using a light microscope and image processing techniques. The nerve fiber diameters were measured and fiber diameter frequency distributions were constructed. In addition the ratio between axon diameter and fiber diameter (a quantity known as g) was derived. The cross-sectional area of each root was measured and in two roots the number of fibers were counted. Preliminary results of this work were reported elsewhere [Rijkhoff et al., 1995].

MATERIALS AND METHODS

Animal Preparation

Two beagle dogs, (dog 1: female, 2.1 years, 13 kg; dog 2: male, 14 years, 16 kg) were used. Under pentobarbital anaesthesia a laminectomy (L4-S2) was performed and the dura was opened to get access to the intradural sacral roots. Intravesical and intraurethral pressure was measured using a transurethral two-point pressure catheter. Identification of the different roots was performed by observing responses such as contraction of hind leg muscles, contraction of the pelvic floor, movement of the tail, and increase of intravesical and intraurethral pressure to electrical stimulation of a complete nerve root using a hook electrode. Stimulation of the S1 roots resulted in flexion of the paw and urethral sphincter contraction. Stimulation of the S2 roots resulted mainly in detrusor and urethral sphincter contraction while stimulation of the S3 roots led solely to movement of the tail. Identification was further helped by size differences (S1 is bigger than S2 and S3). After identification, each root was split in a ventral and dorsal part by tracing the nerves back to their origin at the conus medularis. A suture was placed around the parts to keep all rootlets together. Approximately 2 cm of the intradural root (between conus and dorsal ganglion) was removed for analysis.

Nerve Preparation

The root pieces were fixated in glutaraldehyde, dehydrated with alcohol, and embedded in epon. The myelin was stained with osmium. After hardening 0.5 μm, thick transverse coupes were cut and stained with 1% paraphenileendiamine (1 hour) for extra contrast.

Description of Hardware

For automatic analysis, images were taken of the cross-sections using a system consisting of a light microscope (Zeiss, Thornwood, NY, with $\times 10$ ocular and $\times 2.5$, $\times 10$, $\times 20$, and $\times 40$ objectives), a video camera (HCS-CCD, MXR, Vision Technology, Eindhoven, The Netherlands) with monitor, a 80486-computer, and an image processing board (PCVISIONplus, Vision Technology).

Functionally, an area (e.g., 100×100 μm, using $\times 400$ magnification) of the microscopic image was viewed by the video camera mounted in the vertical tube of the microscope. This image was digitized in a resolution of 512×512 pixels with 256 grey tones and stored on hard disk for later analysis. To determine the cross-sectional area of the roots, images with $\times 25$ magnification (Fig. 1a–d) were used. Morphometric analysis were performed using $\times 400$ magnification (Fig. 2).

Software Algorithms

To determine the cross-sectional area of the roots, software was written that allowed drawing of a closed contour of a cross-section and automatic calculation of the enclosed area. When a root consisted of two or more rootlets, the sum of the rootlet areas was used to obtain the total transverse root area.

Software for morphometric analysis of the digitized images was written in TIM (TEA, Dordrecht, The Netherlands). It calculates for each fiber the axon diameter d and the fiber diameter D (axon + myelin sheath). First the outer and inner border of

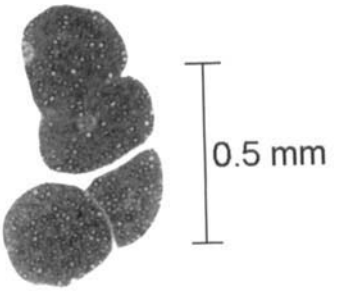

a

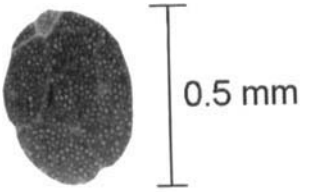

b

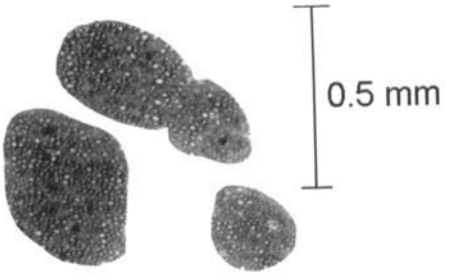

c

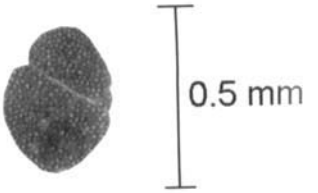

d

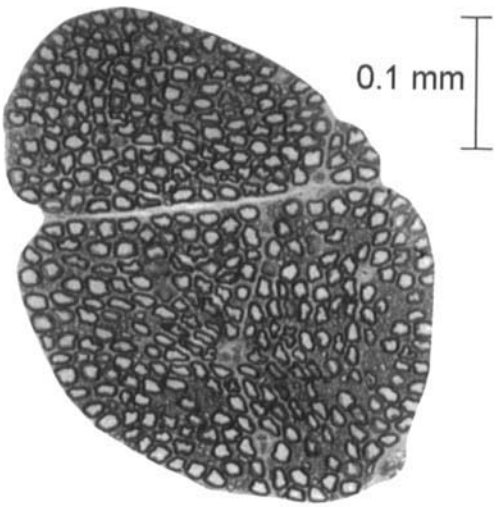

e

Fig. 1. Cross-sections of canine intradural sacral nerve roots. **a:** S2 dorsal; **b:** S2 ventral; **c:** S3 dorsal; **d,e:** S3 ventral. a–d, ×25 magnification; e, ×100 magnification.

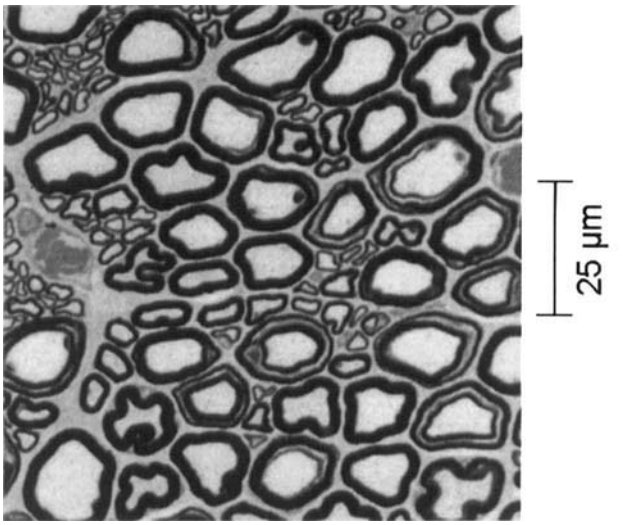

Fig. 2. Example of an image used for morphometric analysis of the cross-section (× 400 magnification).

the myelin is determined. Using these borders the cross-sectional area of the fiber and the axon are calculated. Assuming the calculated areas to be the area of a circle, axon diameter and fiber diameter are derived.

Nerve fiber diameter frequency distributions were constructed by combining the results of several images (7–18, depending on the area of the root) taken at random positions in the cross-section.

Statistics

To determine g (ratio between axon diameter d and fiber diameter D) it was assumed that g is independent of d and D (see Discussion) and that both d and D have the same standard deviation as both variables are measured in the same way. Under these assumptions g can be calculated by minimizing the sum of the distances between the points (d_i, D_i) and the line $d = gD$ [Beck and Arnold, 1977]. This comes down to minimizing $\sum_{i=1}^{N} \frac{gD_i + d_i}{\sqrt{g^2+1}}$ with respect to g, N = number of analyzed fibers in a root.

RESULTS

Intradural nerve roots are composed of tightly packed nerve fibers and a few small blood vessels. In contrast to peripheral nerves, intradural nerve roots have no epineurium and nearly no perineurium. A set of cross-sections, depicted in Figure 1, shows that the ventral roots mostly consist of one unit while the dorsal roots consist of several rootlets. The shape of the ventral roots is somewhat elliptical. An overview of a cross-section at × 100 magnification (Fig. 1e) shows clearly the absence of epineurium.

Figure 3 shows the nerve root cross-sectional areas while Table I contains the

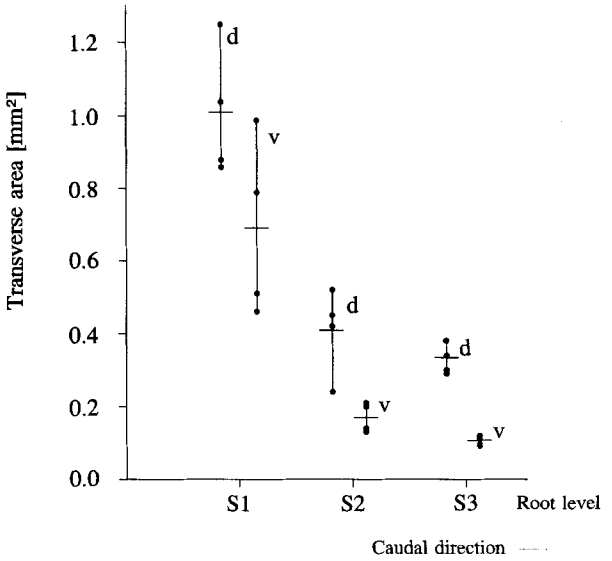

Fig. 3. Cross-sectional area of intradural sacral nerve roots. The transverse areas of the four roots (2 dogs, left and right) at each root level have been depicted by dots which are linked by a vertical bar. The horizontal bar represents the average area of the 4 cross-sections. d = dorsal, v = ventral.

numerical data. The average cross-sectional area of a complete root (dorsal + ventral) decreases in caudal direction (S1: 1.70 mm^2, S2: 0.58 mm^2, S3: 0.43 mm^2). The S1 nerve is the largest sacral root, its cross-sectional area is about three times as large as the cross-sectional area of S2 and S3. The dorsal part of each root is larger than the ventral part and the relative difference in area between dorsal and ventral parts increases in caudal direction. The average area ratio between dorsal and ventral part is 1.54, 2.49, and 3.17 for S1, S2, and S3, respectively. For each root that consisted of only one rootlet, the largest diameter was determined (Table I). If the root consisted of several rootlets an average root diameter was calculated (assuming the root to be circular).

In the two S3 ventral (S3v) roots of the right side, the total number of myelinated fibers with a diameter above ~1.5 μm was counted. The S3v root of dog 1 contained 795 fibers while 559 fibers were counted in the S3v root of dog 2. This resulted in a fiber density of 6.6 * 10^3 fibers/mm^2 for dog 1 and 6.0 * 10^3 fibers/mm^2 for dog 2.

Fiber Diameter Distributions of the Dorsal Roots

An example of an image used for morphometric analyses is shown in Figure 2 while Figure 4 shows the calculated nerve fiber diameter frequency distributions for the S2 and S3 roots. Each bar in the histograms represents the relative frequency of occurrence.

The law of separation of function of spinal roots (law of Bell and Magendie) is, in contrast to humans, valid for dogs. The canine dorsal sacral root fibers are almost all afferent in function, only about 1% are expected to be efferents [Schalow, 1992b].

TABLE I. Cross-Sectional Area and Diameter of S1-S3 Intradural Sacral Nerve Roots

		Cross-sectional area (mm^2)		Diameter (mm)	
		dog 1	dog 2	dog 1	dog 2
S1					
Dorsal	Left	0.88	1.04	1.06[b]	1.15[b]
	Right	0.86	1.25	1.05[b]	1.26[b]
Ventral	Left	0.46	0.79	0.86[a]	1.27[a]
	Right	0.51	0.99	1.05[a]	1.12[b]
S2					
Dorsal	Left	0.24	0.45	0.55[b]	0.76[b]
	Right	0.52	0.42	0.81[b]	0.73[b]
Ventral	Left	0.14	0.21	0.49[a]	0.54[a]
	Right	0.13	0.20	0.47[a]	0.55[a]
S3					
Dorsal	Left	0.38	0.34	0.70[b]	0.66[b]
	Right	0.30	0.29	0.62[b]	0.73[a]
Ventral	Left	0.096	0.11	0.41[a]	0.38[a]
	Right	0.12	0.093	0.45[a]	0.37[a]

[a]When a root consisted of only one rootlet, the largest diameter of the elliptical shaped cross-section has been measured.
[b]When a root consisted of several rootlets, an average diameter has been calculated, assuming that the root is circular.

Thus, as no α-motoneurons are present, one expects the dorsal roots to be mainly composed of small diameter fibers.

The constructed fiber diameter frequency distribution histograms of the S2 dorsal roots (Fig. 4a) have roughly a unimodal distribution. The distributions of all four nerves most often have a peak of fiber diameters in the range of 4–5 μm. Most of the fibers are relatively small, almost half the fibers are smaller than 6 μm (dog 1_{left}: 54.3%, dog 1_{right}: 49.5%, dog 2_{left}: 43.7%, dog 2_{right}: 50.3%). The percentages of large fibers (>12 μm) are 8.8, 9.2, 8.8, and 4.8% for dog 1_{left}, dog 1_{right}, dog 2_{left} and dog 2_{right}, respectively.

The fiber diameter distributions of the S3 dorsal roots (Fig. 4b) also have a unimodal shape, although the distributions of the dog 1 roots have more little peaks. The highest peaks are again in the 4–5 μm range for dog 1. For dog 2 the peaks are in the 5–6 μm range. Again almost half the fibers are smaller than 6 μm (51.7, 39.5, 45.6, and 51.8% for dog 1_{left}, dog 1_{right}, dog 2_{left}, and dog 2_{right}, respectively). For dog 1 the percentages of large fibers (>12 μm) doubled (left: 15.9%, right: 17.9%). For dog 2 the percentages of large fibers are about the same as in the S2 dorsal roots (left: 8.0%, right: 5.1%).

Fiber Diameter Distributions of the Ventral Roots

The canine ventral sacral root fibers are, like the dorsal root fibers, homogeneous in function. Almost all fibers are efferent, only 1% can expected to be afferents [Schalow, 1992b]. Hence, the ventral sacral roots contain the relative large diameter α and γ-motoneurons innervating the muscles of the tail, pelvic floor muscles, and anal and urethral sphincter. The ventral sacral roots also contain the smaller diameter

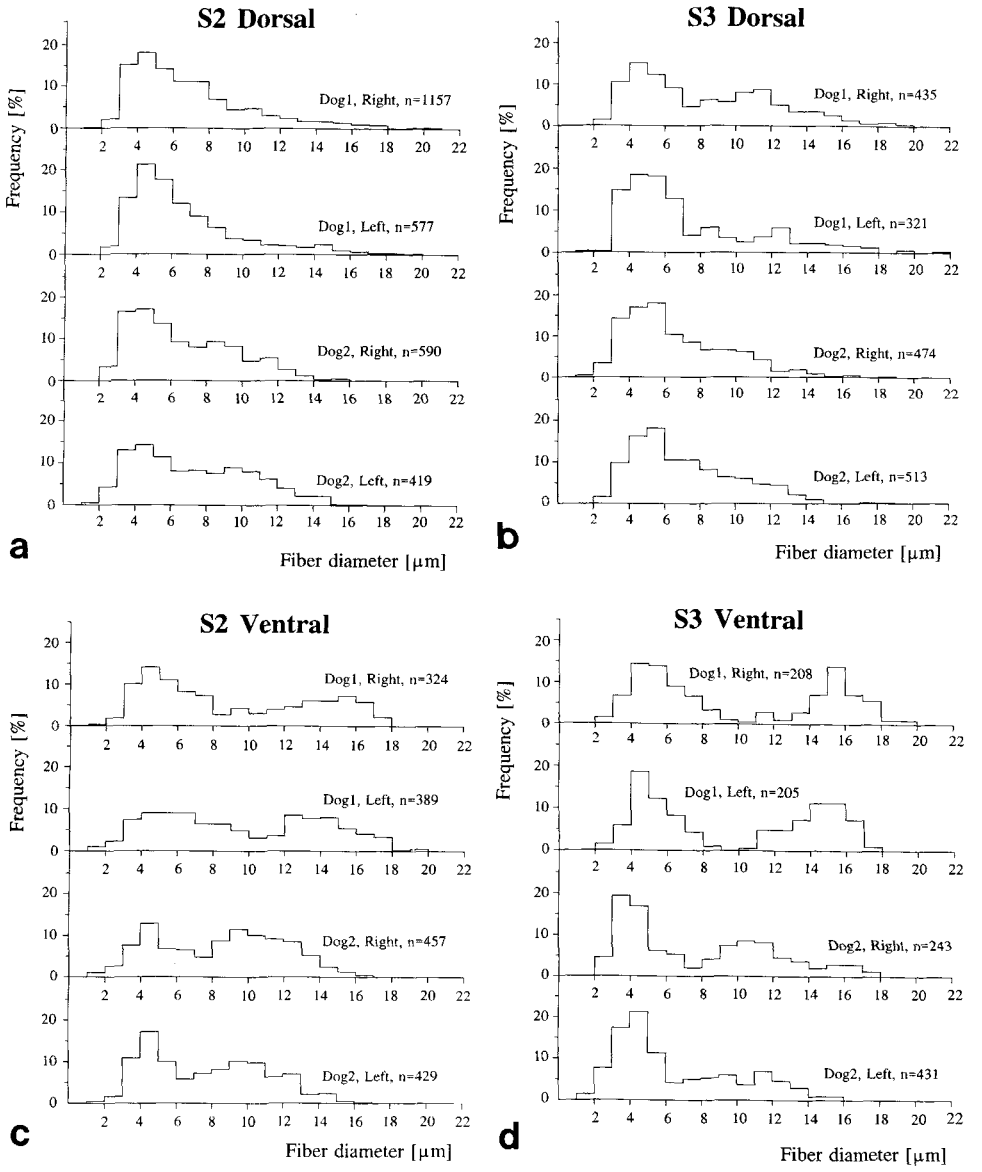

Fig. 4. Myelinated nerve fiber diameter frequency histograms of canine intradural sacral roots. Data of two dogs, two roots (left, right) at each root level. **a:** S2 dorsal; **b:** S3 dorsal; **c:** S2 ventral; **d:** S3 ventral.

preganglionic parasympathetic fibers innervating the bladder and rectum. One would therefore expect a bimodal fiber diameter distribution.

As expected the ventral S2 root fibers do indeed have a diameter distribution with two peaks (Fig. 4c). The first peak is in the range 4–5 μm (dog 1_{left}: 9%, dog 1_{right}: 14.2%, dog 2_{left}: 17.3%, dog 2_{right}: 12.9%) although the dog 1_{left} distribution has a broad top between 4 and 7 μm. The peak in the large fibers is rather flat with a variable position (dog 1_{left}: 12–15 μm, ~8%, dog 1_{right}: 13–16 μm, ~6.5%, dog 2_{left}: 9–11 μm, ~9.9%, dog 2_{right}: 9–11 μm, ~10.8%).

The ventral S3 root fibers also have a bimodal diameter distribution (Fig. 4d). Clear are the peaks of small diameter fibers (dog 1_{left}: 4–5 μm, 18.5%, dog 1_{right}: 4–5 μm, 14.4%, dog 2_{left}: 4–5 μm, 21.4%, dog 2_{right}: 3–4 μm, 19.3%). The large fiber peaks are for dog 1 in the range 14–16 μm (left: 11.2%, right: 13.9%). For dog 2 the peaks are less pronounced and occur at a smaller diameter (10–12 μm, left: 7.0%, right: 8.6%).

Ratio g

The ratio g of axon diameter d to fiber diameter D (axon + myelin) is an important parameter with respect to the internodal conduction time of an action potential. Theoretical analysis of linear cables [Rushton, 1951] predicts a value of 0.6 as the optimum value for the energetically most efficient ratio. Any deviation from this value would increase the internodal conduction time. The ratio g also influences the stimulus needed to excite a fiber. The excitation threshold would decrease with increasing g. Figure 5a and b show in a scatter diagram the relation between D and d for all evaluated fibers of a S2d and a S2v root. The relation appears linear so we chose to fit the line $d = gD + c$ (g = slope, c = intercept) through the points. It turned out that for each root the intercept c was close to zero and that zero was always within the $c \pm$ sd range (sd = standard deviation). Hence a line with zero intercept was fitted as described in the section methods. The results $g \pm$ sd (Table II) show that the calculated ratios g are close to the theoretical optimum of 0.6.

DISCUSSION

Cross-sections of intradural canine sacral nerve roots were analyzed using a light microscope and image processing software. The cross-sectional area of each root was measured and of two cross-sections the total number of fibers was determined. Fiber diameters and axon diameters were determined and used to construct fiber diameter frequency distributions. The work was part of a project with the goal to restore lower urinary tract control by artificial electrical stimulation of the sacral nerve roots.

The results of morphometric analyses could be subjected to dimensional errors, e.g., shrinkage of the material that could be 8% [Dyck et al., 1980; Schnepp et al., 1971]. No attempt was made to correct for these errors.

The cross-sectional area of the S1 roots is clearly larger than the cross-sectional areas of S2 and S3 (Fig. 3). Thus, during operation on the dog, differences in root dimensions can be used for identification of the sacral roots.

If one assumes that the roots are cylindrical then the root diameter can be calculated. These average total diameters (dorsal + ventral) are 1.46, 0.86, and 0.74 mm for S1, S2, and S3, respectively. Li et al. [1995] reported average diameters of 2.0 and 1.5 mm for the extradural S1 and S2 nerve, respectively. This is larger than our findings but they used larger sized dogs (21–36 kg) and extradural roots usually have a larger caliber than the intradural roots since they are surrounded by a protective perineurium. Schalow and Barth [1992] reported diameters of 0.25 and 0.3 mm for canine S3 ventral roots (Alsatian, weight not reported) which is a little smaller than the 0.35 mm (average diameter) we measured.

Average root diameters of 28 humans were reported by Schalow [1985]. He

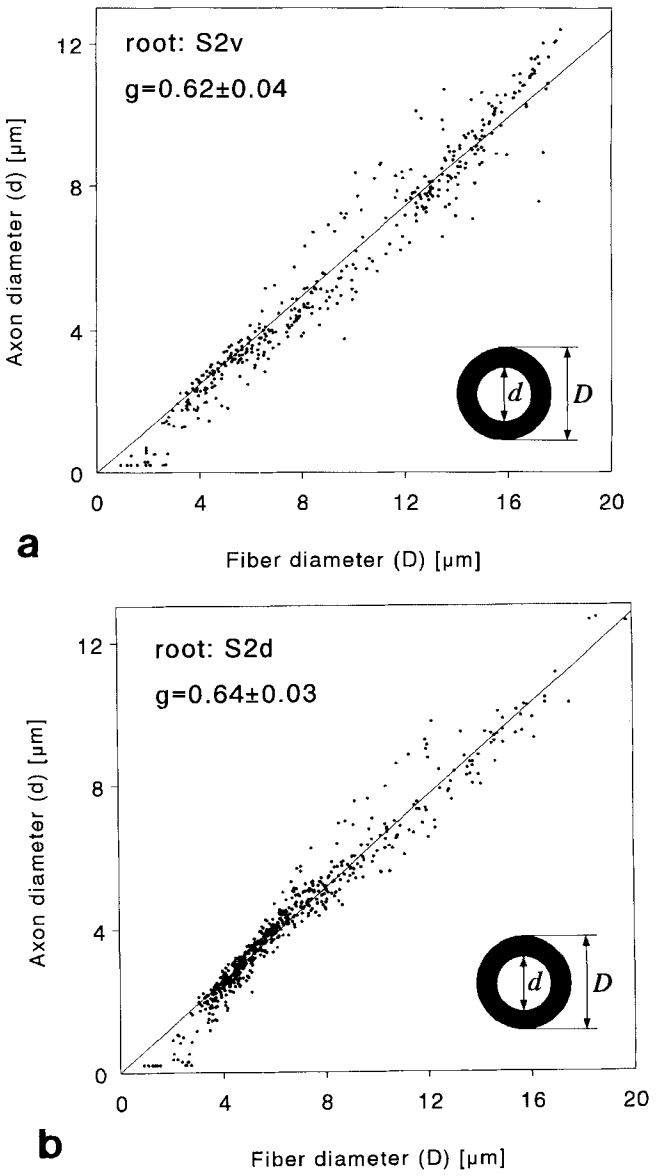

Fig. 5. Scatter diagram of the relation between fiber diameter D and axon diameter d; drawn line represents the estimated ratio g of axon diameter to fiber diameter; **a:** S2 ventral root, number of fibers: 389, g: 0.62 ± 0.04; **b:** S2 dorsal root, number of fibers: 577, g: 0.64 ± 0.03.

measured diameters of 2.6, 2.0, 1.3, and 0.8 mm for the dorsal S1, S2, S3, and S4 roots, respectively. The average values for the ventral roots were 2.0, 1.25, 0.7, and 0.4 mm. Compared to our results of the dog, the diameters of the human S1, S2, and S3 ventral roots are roughly twice as large as in the beagle dog. This means that circumneural electrodes for humans must have a larger inner diameter than the ones used in the beagle dog. Due to the larger electrodes the stimulation currents will be higher in the human than in the dog.

TABLE II. Estimated Ratio $g \pm$ sd (Standard Deviation) of Axon Diameter d to Fiber Diameter D of the Analysed Fibers in a Root

		dog 1		dog 2	
		n	g ± SD	n	g ± SD
S2					
Dorsal	Left	577	0.64 ± 0.03	419	0.59 ± 0.05
	Right	1157	0.64 ± 0.03	590	0.56 ± 0.05
Ventral	Left	389	0.62 ± 0.04	429	0.59 ± 0.07
	Right	324	0.61 ± 0.05	456	0.57 ± 0.07
S3					
Dorsal	Left	321	0.66 ± 0.03	512	0.59 ± 0.05
	Right	435	0.64 ± 0.04	473	0.60 ± 0.05
Ventral	Left	205	0.59 ± 0.05	431	0.57 ± 0.07
	Right	208	0.63 ± 0.03	241	0.65 ± 0.07

*n: number of analyzed fibers in a root.

The axon diameter and fiber diameter of the fibers were calculated by assuming the calculated area of the fiber to be the area of a circle. The actual transverse shape of a fiber is usually not a perfect circle but varies from elliptical to "boomerang" to "star" depending on the position of the transection of the fiber relative to the node of Ranvier. However, Karnes et al. [1977] showed that in non-oblique transverse sections of nerve trunks, the diameter calculated from the measured area converted to a circular shape is the best among various estimates of myelinated fiber diameters and is the most suitable one in computerized morphometric analysis.

The number of automatically analyzed fibers, shown in Figure 4a–d, is less than the total number of fibers visible in the images. Fibers have been omitted from analyses if they bear artifacts such as holes in the myelin. Those artifacts seem to occur in the whole diameter range so we assume that the introduced error in the fiber diameter distributions will be small.

Schalow and Barth [1992] have presented the diameter distribution of a canine sacral ventral root. They found a bimodal distribution with peaks of most occurring fiber diameters at the ranges 5–6 and 13–17 μm. This agrees with our results (Fig. 4d). The diameter distributions of the dorsal root fibers are very much alike in both dogs. The distributions of the ventral root fibers are also alike (bimodal) but the distance between the peaks differs. In dog 1 the peaks are more separated than in dog 2. This could be due to the age difference of the dogs.

To control the lower urinary tract in spinal cord injury by electrical stimulation of the sacral roots, selective activation of detrusor and urethral sphincter is only possible if the innervating nerve fibers differ in diameter. The obtainable selectivity by electrical stimulation increases with increasing difference in diameter between the two fiber groups. This implies that independent activation of both large and small fibers would be less easy in the old dog. This was confirmed in experiments.

Both human and canine ventral sacral roots have a fiber diameter distribution with a bimodal shape with peaks of most occurring fiber diameters at approximately the same position (parasympathetic fibers: 3–5 μm; somatic fibers: 13–15 μm). However, the canine ventral sacral roots contain relatively more large diameter fibers than human ventral sacral roots as the canine ventral sacral roots contain also the

fibers innervating muscles of the tail. This is confirmed by comparing the canine data with human data presented by Schalow and co-workers. A nerve fiber diameter distribution histogram of a human S4 ventral root [Fig. 8 in Schalow, 1989] shows that 67% of all myelinated fibers were of a small caliber (1–6 μm) and that only 16% were of a large caliber (>10 μm). The diameter distribution of another human S4 ventral root [Schalow et al., 1995] showed that 77% of all myelinated fibers were of a small caliber (1.5–6 μm). In the comparable S3 canine ventral roots only 50–60% are of a small caliber (Fig. 4d).

The composition of the dorsal roots could not be compared since detailed information on the composition of human dorsal sacral roots is not available in the literature, but no large differences are expected.

A nerve fiber density of $9.0 * 10^3$ myelinated nerve fibers/mm^2 has been reported for human sacral ventral roots [Schalow et al., 1987]. But, as the canine ventral sacral roots contain relatively more larger fibers than the human sacral roots the fiber density in the canine ventral sacral roots is expected to be less the fiber density in the human sacral ventral roots. The calculated nerve fiber density of the two canine S3 ventral roots ($6.0 * 10^3$ and $6.6 * 10^3$ fibers/mm^2) is therefore in line with the expectations.

To determine the ratio g we assumed it to be independent of d and D, which is not generally agreed upon. Some reports show a rising g with increasing D and reaching a plateau while other reports show a continuous rising g with increasing D. This issue has been addressed by Williams and Wendell-Smith [1971] who conclude that those differences are caused by errors in the mensuration of the fibers. The work of Schnepp and Schnepp [1971] showed a ratio of 0.6 which was practically constant over a wide range of fiber diameters in various mammals. Therefore we assumed g to be independent of D. Our calculated ratios vary from 0.56 ± 0.05 to 0.66 ± 0.03 (mean ± sd) which is close to the theoretical optimum value of 0.6 for the energetically most efficient ratio [Rushton, 1951].

In conclusion, the fiber diameter distributions and nerve fiber densities of the human and the dog sacral nerves are similar so the dog is a satisfactory model for electrical sacral root stimulation research. The presented data will help to improve the understanding of the experimental results on sacral root stimulation and will lead to optimization of the stimulation patterns.

ACKNOWLEDGMENT

The work described in this article was supported by the Dutch Kidney Foundation C92.1249.

REFERENCES

Beck JV, Arnold KJ (1977): "Parameter Estimation in Engineering and Science." New York: John Wiley & Sons, pp 198–199.

Brindley GS, Polkey CE, Rushton DN, Cardozo L (1986): Sacral anterior root stimulators for bladder control in paraplegia: The first 50 cases. J Neurol Neurosurg Psychiatry 49:1104–1114.

Carlsson C-A, Sundin T (1980): Reconstruction of afferent and efferent nervous pathways to the urinary bladder in two paraplegic patients. Spine 5:37–41.

Dyck PJ Low, PA, Spacks MF, Hexum LA, Karnes JL (1980): Effect of serum hyperosmolarity of healthy human sural nerve. J Neuropathol Exp Neurol 39:285–295.

Hohenfellner M, Paick J-S, Trigo-Rocha F, Schmidt RA, Kaula NF, Thüroff JW, Tanagho EA (1992): Site of deafferentation and electrode placement for bladder stimulation: Clinical implications. J Urol 147:1665–1670.

Hosein RA, Griffiths DJ (1990): Computer simulation of the neural control of bladder and the urethra. Neurourol Urodyn 9:601–618.

Ishigooka M, Hashimoto T, Sasagawa I, Izumiya K, Nakada T (1994): Modulation of the urethral pressure by high-frequency block stimulus in dogs. Eur Urol 25:334–337.

Karnes J, Robb R, O'Brien PC, Lambert EH, Dyck PJ (1977): Computerized recognition for morphometry of nerve attribute of shape of sampled transverse sections of myelinated fibers which best estimates their average diameter. J Neurol Sci 34:43–51.

Koldewijn EL, Rosier PFWM, Meuleman EJH, Koster AM, Debruyne FMJ, van Kerrebroeck PEV (1994): Predictors of success with neuromodulation in lower urinary tract dysfunction. J Urol 152: 2071–2075.

Li J-S, Hassouna M, Sawan M, Duval F, Elhilali MM (1992): Electrical stimulation induced sphincter fatigue during voiding. J Urol 148:949–952.

Li J-S, Hassouna M, Sawan M, Duval F, Elhilali MM (1995): Long-term effect of sphincteric fatigue during bladder neurostimulation. J Urol 153:238–242.

Rijkhoff NJM, Holsheimer J, Koldewijn EL, Struijk JJ, van Kerrebroeck PEV, Debruyne FMJ, Wijkstra H (1994a): Selective stimulation of sacral nerve roots for bladder control; A study by computer modeling. IEEE Trans Biomed Eng 41:413–424.

Rijkhoff NJM, Koldewijn EL, van Kerrebroeck PEV, Debruyne FMJ, Wijkstra H (1994b): Acute animal studies on the use of an anodal block to reduce urethral resistance in sacral root stimulation. IEEE Trans Rehab Eng 2:92–99.

Rijkhoff NJM, d'Hollosy W, Debruyne FMJ, Wijkstra H (1995): Morphometric canine sacral root data. Proc 3rd Int Congr Dutch Urol Assoc, Nov. 1–3, Nijmegen, The Netherlands, p 78.

Rushton WAH (1951): A theory of the effects of fiber size in medullated nerve. J Physiol 115:101–122.

Schalow G (1985): The problem of cauda equina nerve root identification. Zentralbl Neurochir 46:322–330.

Schalow G (1989): Efferent and afferent fibers in human sacral ventral nerve roots: Basic research and clinical implications. Electromyogr Clin Neurophysiol 29:33–53.

Schalow G (1992a): Number of fibres and fibre diameter distributions of nerves innervating the urinary bladder in humans. Acceptor nerve analysis (IV). Electromyogr Clin Neurophysiol 32:187–196.

Schalow G (1992b): Ventral root afferent and dorsal root efferent fibres in dog and human lower sacral nerve roots. Gen Physiol Biophys 11:123–131.

Schalow G, Barth H (1992): Group conduction velocities and nerve fibre diameters of α and γ-motoneurons from lower sacral nerve roots of the dog and humans. Gen Physiol Biophys 11:85–99.

Schalow G, Aho A, Lang G (1987): Nerve fiber counts for an intercostal nerve to cauda equina root anastomosis. Zentralbl Chir 112:457–461.

Schalow G, Zäch GA, Warzok R (1995): Classification of human peripheral nerve fibre groups by conduction velocity and nerve fibre diameter is preserved following spinal cord lesion. J Autonom Nerv Syst 52:125–150.

Schmidt RA (1988): Applications of neurostimulation in urology. Neurourol Urodyn 7:484–592.

Schmidt RA, Bruschini H, Tanagho EA (1979): Sacral root stimulation in controlled micturition. (Peripheral somatic neurotomy and stimulated voiding). Invest Urol 17:130–134.

Schnepp P, Schnepp G (1971): Faseranalytische untersuchungen an peripheren nerven bei tieren verschiedener größe. II Verhaltnis axondurchmesser/gesamtdurchmesser und internodallänge. Z Zellforsch 119:99–114.

Schnepp P, Schnepp G, Spaan G (1971): Faseranalytische untersuchungen an peripheren nerven bei tieren verschiedener größe. I Fasergesamtzahl, Faserkaliber und nervenleitungsgeschwindigkeit. Z Zellforsch 119:77–98.

Siegel SW (1992): Management of the voiding dysfunction with an implantable neuroprosthesis. Urol Clin North Am 19:163–170.

Sweeney JD, Mortimer JT, Bodner DR (1990): Animal study of pudendal nerve cuff electrode implants for collision block of motor activity. Neurourol Urodyn 9:83–93.

Thüroff JW, Bazeed MA, Schmidt RA, Wiggin DM, Tanagho EA (1982): Functional pattern of sacral root stimulation in dogs: II Urethral closure. J Urol 127:1034–1038.

van Kerrebroeck PEV, Koldewijn E, Wijkstra H, Debruyne FMJ (1991): Intradural sacral rhizotomies and

implantation of an anterior sacral root stimulator in the treatment of neurogenic bladder dysfunction after spinal cord injury; Surgical technique and complications. World J Urol 9:126–132.
Williams PL, Wendell-Smith CP (1971): Some additional parametric variations between peripheral nerve fiber populations. J Anat 109:505–526.